



Plant Archives

Journal homepage: <http://www.plantarchives.org>

DOI Url : <https://doi.org/10.51470/PLANTARCHIVES.2025.v25.no.1.282>

IN SILICO IDENTIFICATION OF ANTIVIRAL COMPOUNDS FROM GENUS *ASPARAGUS* FOR CHIKUNGUNYA VIRUS USING MOLECULAR DOCKING AND MD SIMULATION

Aman Agrawal¹, Deepti Teotia¹, Vivek Kumar¹, Pooja Jain¹, Bhanu Agrawal² Ashish Kumar¹ and Vijai Malik^{1*}

¹Department of Botany, Chaudhary Charan Singh University, Meerut U.P. India (250004)

²B.S.A. (PG) College, Dr. Bhim Rao Ambedkar University, Agra U.P. India (282004)

*Corresponding author E-mail: vijaimalik1973@gmail.com

(Date of Receiving : 15-01-2025; Date of Acceptance : 16-04-2025)

ABSTRACT

The cases of chikungunya have been documented worldwide since the last 20 years of the current century. Effective medications or vaccines to cure chikungunya are not available. The desirable target of inhibitors is non-structural protein nsP2 cysteine protease (nsP2pro). The nsP2pro is a crucial enzyme that catalyses the proteolytic cleavage of polyprotein precursors that generate functional proteins essential for the virus's reproduction and growth. In the present study strong & non-toxic natural inhibitors bioactive compounds from *Asparagus racemosus* and *Asparagus officinalis* were chosen in order to target nsP2pro for curing chikungunya. Out of fifty metabolite, thirty-six metabolite of *A. racemosus* and *A. officinalis* possessed the criteria for drug likeness. AutoDock vina was used to conduct a virtual screening of 36 chosen compounds. COUMESTROL molecules that had the lowest binding energy (-6.8) was selected for further analysis. MMPBSA and molecular dynamics simulation were applied to coumestrol metabolites, and RMSD, RMSF, Rg, SASA, and hydrogen bonding were used to evaluate the robustness of protein-ligand complexes.

Keywords: *Asparagus*, Chikungunya Virus, nsP2 Cysteine Protease, Molecular Docking, Molecular Dynamics Simulation, MMPBSA.

Introduction

Chikungunya was first identified from southern Tanzania in 1952 (Ross, 1956). It is characterized by abrupt fever mostly accompanied by joint pain. The symptoms may continue for a few days and occasionally stay for weeks, months, or even years. Additional manifestations comprise muscular pain, swelling at joints, nausea, headache, rash, and fatigue (Robinson, 1955). Chikungunya virus (CHIKV), the causal agent of chikungunya, is a member of the family Togaviridae and belongs to the genus Alphavirus (Van Bortel *et al.*, 2014). From 2007 to 2012, 231 cases of chikungunya were reported in Italy, Europe (Tomasello & Schlagenhauf, 2013). In 2014, Europe experienced the highest burden of chikungunya, with approximately 17,000 reported cases (Van Bortel *et al.*, 2014). India reported 18,639 cases in 2013 (Cecilia, 2014), while Pakistan documented 4,000 cases in 2016 (Rauf *et al.*,

2017). The mosquitoes *Aedes aegyptian* and *A. albopictus*, which are known to be the most anthropophilic mosquitoes with a close relationship to people, were shown to be the virus's vectors. Once infected, they bite humans and transfer the virus directly into the circulation (Van Bortel *et al.*, 2014). This virus is an icosahedral, enclosed entity that measures 65–70 nm in diameter. Its positive-sense ssRNA makes up roughly 11.8 Kb of its genome. The genome translates into nine proteins, classified into two types of proteins, i.e. structural and non-structural proteins. Five structural proteins include one capsid (C), two envelope glycoproteins E1 and E2 and two smaller peptides E3 and SP6K, while four non-structural proteins are nsP1, nsP2, nsP3 and nsP4 (Singh *et al.*, 2018). Two ORFs are present in the viral genome, one of which codes for nonstructural proteins that begin synthesis as soon as the virus enters a host

cell. Viral-encoded nsP2 cysteine protease (nsP2pro) further processed the nonstructural polyprotein precursor by proteolytic cleavage into constituent nonstructural proteins nsP1, nsP2, nsP3, and nsP4. These nonstructural proteins are essential for the replication of the viral genome and subgenomic expression (Kumar *et al.*, 2023). A two-domain protein with several functions is called nsP2pro. While polyprotein cleavage into constituent nsPs is attributed to the C-terminal domain, RNA helicase, RNA dependent 5'-triphosphatase, and nucleoside triphosphatase activities are attributed to the N-terminal domain (Rikkonen, 1996). Cys478-His548 is the catalytic dyad of nsP2pro. The most conserved residue in alpha viruses is Trp549. Drugs and inhibitors find the C-terminal domain of nsP2 to be an appealing target because it is essential to the viral replication cycle (Narwal *et al.*, 2018). Furthermore, nsP2 protease reaches the host cell's nucleus and inhibits the production of antiviral genes (Fros *et al.*, 2010). There is currently no effective medication or vaccination to treat CHIKV.

Medicinal plants occupy an important position in the socio-cultural, spiritual and medicinal arena of India and in many countries of Asia, Africa and East Europea are needs for primary health care (Jain *et al.*, 2024; Farnsworth *et al.*, 1985 & Teotia *et al.*, 2024). Out of about 250,000 flowering plants of the world, more than 50,000 are used for medicinal purposes (Hasan *et al.*, 2016). The genus *Asparagus* (family Asparagaceae) comprises approximately 300 species distributed globally, with 22 species found in India. Among these, *Asparagus racemosus* is the most commonly utilized in traditional medicine (Bopana & Saxena, 2007), while *Asparagus officinalis* is used in the treatment of various diseases, demonstrating anti-inflammatory, analgesic, and anti-arthritic activities (Kumar *et al.*, 2023). This prompted the use of an in silico method to evaluate the bioactive metabolites against chikungunya virus. In the present work, we investigated the potential inhibiting efficiency of selected bioactive metabolites from different *Asparagus racemosus* and *Asparagus officinalis* to the nsP2pro, an important enzyme involved in the processing of nonstructural polyprotein complex, using molecular docking, atomistic explicit solvent MD simulations (molecular dynamic simulations), and MMPBSA (Molecular Mechanics Poisson Boltzmann Surface Area) based free energy calculations.

Materials and Methods

Metabolite library

A library of 36 structurally distinct phytomolecules was created from an initial pool of 50 metabolites (supplementary table 1) for the identification of potential CHIKV therapies. The chemical and structural characteristics of these metabolites, including molecular weight, chemical formula, and canonical SMILES, were obtained from the PubChem Database (Kim *et al.*, 2019).

ADME analysis

The Swiss ADME tool was utilised to compute the ADME (absorption, distribution, metabolism, and excretion) characteristics of phytomolecules (Swiss ADME, 2017). Lipinski's rule of five establishes the pharmacokinetic and pharmacodynamic features of the compounds (Lipinski *et al.*, 1997). For the purpose of docking experiments, 36 compounds were chosen based on specific drug likeliness characteristics.

Protein and ligand preparation

The CHIKV protease's 3D coordinates (PDB ID 4ZTB) with resolution 2.59 Å was taken from RCSB database (<http://www.rcsb.org/pdb/home/home.do>). Protein optimisation and energy-minimization was done using SPDBV software. This was then saved in PDB format (Guex & Peitsch, 1997). Using the Autodock4.2 programme, the hydrogen atoms and Kollman charges were added, and the file was saved in pdbqt format (Morris *et al.*, 2009). Phytochemicals were retrieved from pub-chem database and downloaded in 3D SDF format (Kim *et al.*, 2019). Using the OpenBabel programme, 3D SDF structures of phytochemicals were converted in PBD format using canonical smiles. Using the steepest descent technique of the Open Babel tools, energy reduction and optimisation of molecules were completed in the Linux interface and saved in the pdbqt format (O'Boyle *et al.*, 2011).

Molecular docking studies

Using Auto-Dock Vina, molecular docking was used to identify putative antiviral compounds (Trott & Olson 2010). The values for the grid centre point were adjusted X = 20.223, Y = 1.321, and Z = -16.419. The measurements of the box were 16 Å × 16 Å × 16 Å. Rest of the parameters were maintained as default. The distribution of binding energy ranged from -2.7 to -6.8 kcal/mol. The compounds selected for molecular dynamics simulation (MD simulation) have lowest binding energies of -6.8 kcal/mol. Using the receptor-ligand interactions module of Discovery Studio 2D and

3D interactions of certain complexes were analysed (Design, 2014).

Molecular Dynamics simulation analysis

To assess the dynamic properties of the phytomolecule-protein complexes, MD simulation simulations were conducted. The Charmm36-feb 2021.ff force field was utilised in all simulations (Vanommeslaeghe *et al.*, 2010) using GROMACS 2020.1-1 version (Van Der Spoel *et al.*, 2005). The ligand topology files were created using the CGenFF server (Vanommeslaeghe *et al.*, 2010). Protein complexes that had been created were solved in a cubic box, and enough ions were added to keep the system neutral. The steepest descent approach was used to minimise the system's energy with a convergence threshold of less than 1000 kJ/mol/nm in order to remove any steric collisions among atoms. After system relaxation equilibration was carried out in two stages. A constant number, volume, and temperature (NVT) simulation was performed for 100 ns at a temperature of 300 K and the coordinates were saved. After temperature stability was attained, a constant number, pressure, and temperature (NPT) simulation was performed for 100 ns. During this phase of the simulation, the temperature was set to 300 K and the pressure to 1 bar, with coupling constant of 0.1 and 0.1 ps respectively. The solvent and ions were kept unrestrained in the NVT ensemble for 100ns in the first phase, while the restraint weight from the protein and protein-ligand complexes was gradually reduced in the NPT ensemble for 100ns in the second phase. The LINCS algorithm was used to keep all hydrogen bonds constrained (Hess *et al.*, 1997). Utilizing Berendsen's temperature and Parrinello-Rahman pressure coupling, the temperature and pressure of the system were kept at 300 K and 1 atm respectively (Berendsen *et al.*, 1984). MD simulation trajectory was analyzed by the available GROMACS program and Python-3.8 scripts.

MMPBSA free energy calculation

MMPBSA was used to calculate the binding energy and the energy contribution per residue. In MMPBSA, the nonpolar component (ΔG_{npolv}) was computed using a linear connection to the solvent accessible surface area (SASA), whereas the polar percentage of solvation energy (ΔG_{psolv}) was evaluated by solving the Poisson-Boltzmann equation. In this study, different parts of the binding free energy of complexes were estimated using the gmmPBSA module of GROMACS (Kumari *et al.*, 2014). The 100ns of the trajectory were used in the analysis.

Results and Discussion

Drug likeliness properties

Numerous physicochemical and functional parameters that influence a given molecule's likely drug-like behaviour are taken into account in silico drug-likeness assessments. In contrast, the pharmacophoric characters determine the molecular interaction with the living system through transport, absorption, metabolic stability, distribution, affinity to proteins, reactivity, toxicity, etc. The physicochemical characters primarily include molecule size, molecular flexibility, lipophilicity, electronic distribution, and hydrogen bonding characteristics. By leveraging this information, analysis of molecules can be done with less effort while screening a larger pool of metabolites and with a lower chance of in vivo experiment failure. Of the library's 36 molecules, none violated Lipinski's rule of five (Lipinski *et al.*, 1997) (supplementary table S1). Out of 50 selected secondary metabolites only 36 compounds follow Lipinski's rule of five. All these compounds were further used for molecular docking studies. Selected secondary metabolites with their compound ID, molecular weight, molecular formula & canonical smiles are presented in table 1.

Table 1: Secondary metabolites library with their CID, molecular weight, molecular formula & canonical smiles of Genus *A. racemosus* and *A. officinalis*.

Pub Chem CID	Secondary metabolites name	Molecular weight	Molecular formula	Canonical smile	References
1000	Phenyl ethanolamine (<i>A. officinalis</i>)	137.18g/mol	C ₈ H ₁₁ NO	C1=CC=C(C=C1)C(CN)O	López <i>et al.</i> , 1996
1017	Phthalic acid (<i>A. racemosus</i>)	166.13g/mol	C ₈ H ₆ O ₄	C1=CC=C(C(=C1)C(=O)O)C(=O)O	Thakur <i>et al.</i> , 2018
10742	Syringic acid (<i>A. racemosus</i>)	198.17g/mol	C ₉ H ₁₀ O ₅	COC1=CC(=CC(=C1O)OC)C(=O)O	Hamdi <i>et al.</i> , 2021
11385250	Asparacosin A	444.6g/mol	C ₂₇ H ₄₀ O ₅	CC1CCC2(C(C3(C(O2)CC4	Jang <i>et al.</i> , 2004

	(<i>A. officinalis</i>)			C3(C(CC5C4CCC6=CC(=O)CCC56C)O)C)OC1	
118284	Blumenol C (<i>A. officinalis</i>)	210.31g/mol	C ₁₃ H ₂₂ O ₂	CC1=CC(=O)CC(C1CCC(C)O)(C)C	Jang <i>et al.</i> , 2004
1183	Vanillin (<i>A. racemosus</i>)	152.15g/mol	C ₈ H ₈ O ₃	COC1=C(C=CC(=C1)C=O)O	Hamdi <i>et al.</i> , 2021
131753100	Asparenyol (<i>A. officinalis</i>)	280.3g/mol	C ₁₈ H ₁₆ O ₃	COC1=CC=C(C=C1)OCC=CC#CC2=CC=C(C=C2)O	Terada & Kamisako, 1999
13442868	(S)-(-)-1,2,4-Butanetriol,2-acetate (<i>A. racemosus</i>)	148.16g/mol	C ₆ H ₁₂ O ₄	CC(=O)OC(CCO)CO	Dhanusha <i>et al.</i> , 2021
16682	Asparaguisic acid (<i>A. racemosus</i>)	150.2g/mol	C ₄ H ₆ O ₂ S ₂	C1C(CSS1)C(=O)O	Karthikeyan <i>et al.</i> , 2018
178	Ethanimidic acid (<i>A. racemosus</i>)	59.07g/mol	C ₂ H ₅ NO	CC(=O)N	Agrawal <i>et al.</i> , 2018
180	2-propanone (<i>A. racemosus</i>)	58.08g/mol	C ₃ H ₆ O	CC(=O)C	Sivakumar & Gajalakshmi, 2014
237332	5Hydroxymethylfurfural (<i>A. officinalis</i>)	126.11g/mol	C ₆ H ₆ O ₃	C1=C(OC(=C1)C=O)CO	Ito <i>et al.</i> , 2013
240	Benzaldehyde (<i>A. officinalis</i>)	106.12g/mol	C ₇ H ₆ O	C1=CC=C(C=C1)C=O	Yang <i>et al.</i> , 2022
25310	L-Rhamnose (<i>A. racemosus</i>)	164.16g/mol	C ₆ H ₁₂ O ₅	CC1C(C(C(C(O1)O)O)O)O	Sharma <i>et al.</i> , 1983
40634	Trolox (<i>A. officinalis</i>)	250.29g/mol	C ₁₄ H ₁₈ O ₄	CC1=C(C2=C(CCC(O2)(C)C(=O)O)C(=C1O)C)C	Sun <i>et al.</i> , 2007
439246	Naringenin (<i>A. racemosus</i>)	272.25g/mol	C ₁₅ H ₁₂ O ₅	C1C(OC2=CC(=CC(=C2C1=O)O)O)C3=CC=C(C=C3)O	Hamdi <i>et al.</i> , 2021
439533	Taxifolin (<i>A. officinalis</i>)	304.25g/mol	C ₁₅ H ₁₂ O ₇	C1=CC(=C(C=C1)C2C(C(=O)C3=C(C=C(C=C3O2)O)O)O)O	Zhang <i>et al.</i> , 2020
444972	Fumaric acid (<i>A. officinalis</i>)	116.07g/mol	C ₄ H ₄ O ₄	C(=CC(=O)O)C(=O)O	Hartung <i>et al.</i> , 1990
445858	Ferulic Acid (<i>A. racemosus</i>)	194.18g/mol	C ₁₀ H ₁₀ O ₄	COC1=C(C=CC(=C1)C=CC(=O)O)O	Hamdi <i>et al.</i> , 2021
521314	Myrtanol (<i>A. officinalis</i>)	154.25g/mol	C ₁₀ H ₁₈ O	CC1(C2CCC(C1C2)CO)C	Kadhim & Salah, 2014
5280443	Apigenin (<i>A. racemosus</i>)	270.24g/mol	C ₁₅ H ₁₀ O ₅	C1=CC(=CC=C1C2=CC(=O)C3=C(C=C(C=C3O2)O)O)O	Bajpai <i>et al.</i> , 2022
5280961	Genistein (<i>A. officinalis</i>)	270.24g/mol	C ₁₅ H ₁₀ O ₅	C1=CC(=CC=C1C2=COC3=CC(=CC(=C3C2=O)O)O)O	Zhang <i>et al.</i> , 2020
5281605	Baicalein (<i>A. officinalis</i>)	270.24g/mol	C ₁₅ H ₁₀ O ₅	C1=CC=C(C=C1)C2=CC(=O)C3=C(O2)C=C(C(=C3O)O)O	Zhang <i>et al.</i> , 2019
5281607	Chrysin (<i>A. officinalis</i>)	254.24g/mol	C ₁₅ H ₁₀ O ₄	C1=CC=C(C=C1)C2=CC(=O)C3=C(C=C(C=C3O2)O)O	Zhang <i>et al.</i> , 2020
5281654	Isorhamnetin (<i>A. racemosus</i>)	316.26g/mol	C ₁₆ H ₁₂ O ₇	COC1=C(C=CC(=C1)C2=C(C(=O)C3=C(C=C(C=C3O2)O)O)O)O	Jiang <i>et al.</i> , 2015
5281707	Coumestrol (<i>A. officinalis</i>)	268.22g/mol	C ₁₅ H ₈ O ₅	C1=CC2=C(C=C1O)OC3=C2C(=O)OC4=C3C=CC(=C4)O	Ji <i>et al.</i> , 2016

5281708	Daidzein (<i>A. officinalis</i>)	254.24g/mol	C ₁₅ H ₁₀ O ₄	C1=CC(=CC=C1C2=COC3=C(C2=O)C=CC(=C3)O)O	Zhang et al., 2020
5352586	3-Methyl-1-Cyclooctene (<i>A. racemosus</i>)	124.22g/mol	C ₉ H ₁₆	CC1CCCCC=C1	Thakur et al., 2018
1322	1,2Dimethyl Hydrazine (<i>A. racemosus</i>)	60.1g/mol	C ₂ H ₈ N ₂	CN(C)N	Bongirwar & Tirgar, 2023
637542	p-coumaric acid (<i>A. racemosus</i>)	164.16g/mol	C ₉ H ₈ O ₃	C1=CC(=CC=C1C=CC(=O)O)O	Hamdi et al., 2021
6552009	Borneol (<i>A. officinalis</i>)	154.25g/mol	C ₁₀ H ₁₈ O	CC1(C2CCC1(C(C2)O)C)C	Kadhim & Salah, 2014
72	Protocatechuic acid (<i>A. racemosus</i>)	154.12g/mol	C ₇ H ₆ O ₄	C1=CC(=C(C=C1C(=O)O)O)O	Hamdi et al., 2021
72418	Tetranorlipoic acid (<i>A. racemosus</i>)	150.2g/mol	C ₄ H ₆ O ₂ S ₂	C1CSSC1C(=O)O	Janani & Singaravadiel, 2014
7362	2-Furaldehyde (<i>A. racemosus</i>)	96.08g/mol	C ₅ H ₄ O ₂	C1=COC(=C1)C=O	Agrawal et al., 2018
8175	Decanal (<i>A. racemosus</i>)	156.26g/mol	C ₁₀ H ₂₀ O	CCCCCCCCC=O	Thakur et al., 2018
8184	1-Undecanol (<i>A. racemosus</i>)	172.31g/mol	C ₁₁ H ₂₄ O	CCCCCCCCCCCO	Thakur et al., 2018

Molecular docking analysis

Out of 36 compounds docked by using Autodock Vina, only 31 compounds show their binding interaction with nsP2pro. The binding energy of 31 phytomolecules with nps2 protease was ranges from -2.6 to -6.8 kcal/mol (Fig.1). Nine molecules with highest minimum binding energies are taxifolin (-6.3 kcal/mol) asparenyol, naringenin, apigenin, and isorhamnetin (-6.4 kcal/mol) genistein, baicalein,

daidzein (-6.5kcal/mol) and coumestrol (-6.8kcal/mol) (Fig.1). These molecules form H-bonds, van der Waals forces, pi-pi, pi-Sigma, and pi-alkyl interactions with active site residues of nsP2pro. The interaction analysis also revealed that these molecules interact preferably with Tyr 544 of nsp2pro. The catalytic residue Trp512, and Cys478 of nsp2pro are involved in substrate binding and recognition (table 2).

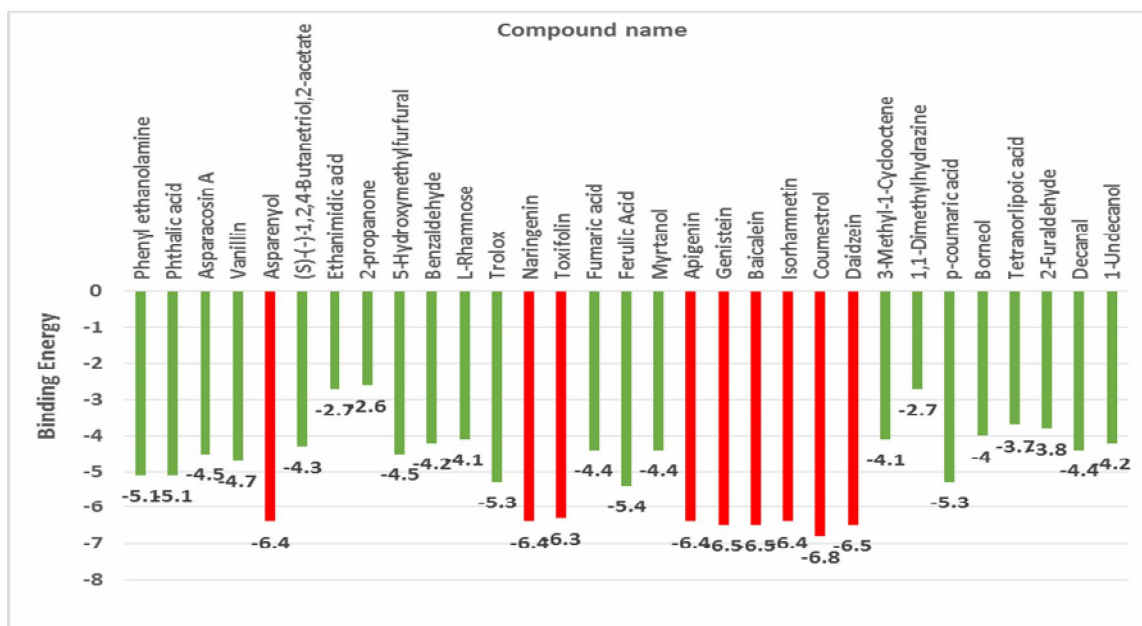


Fig. 1 : Binding energy of selected compounds against nsP2pro

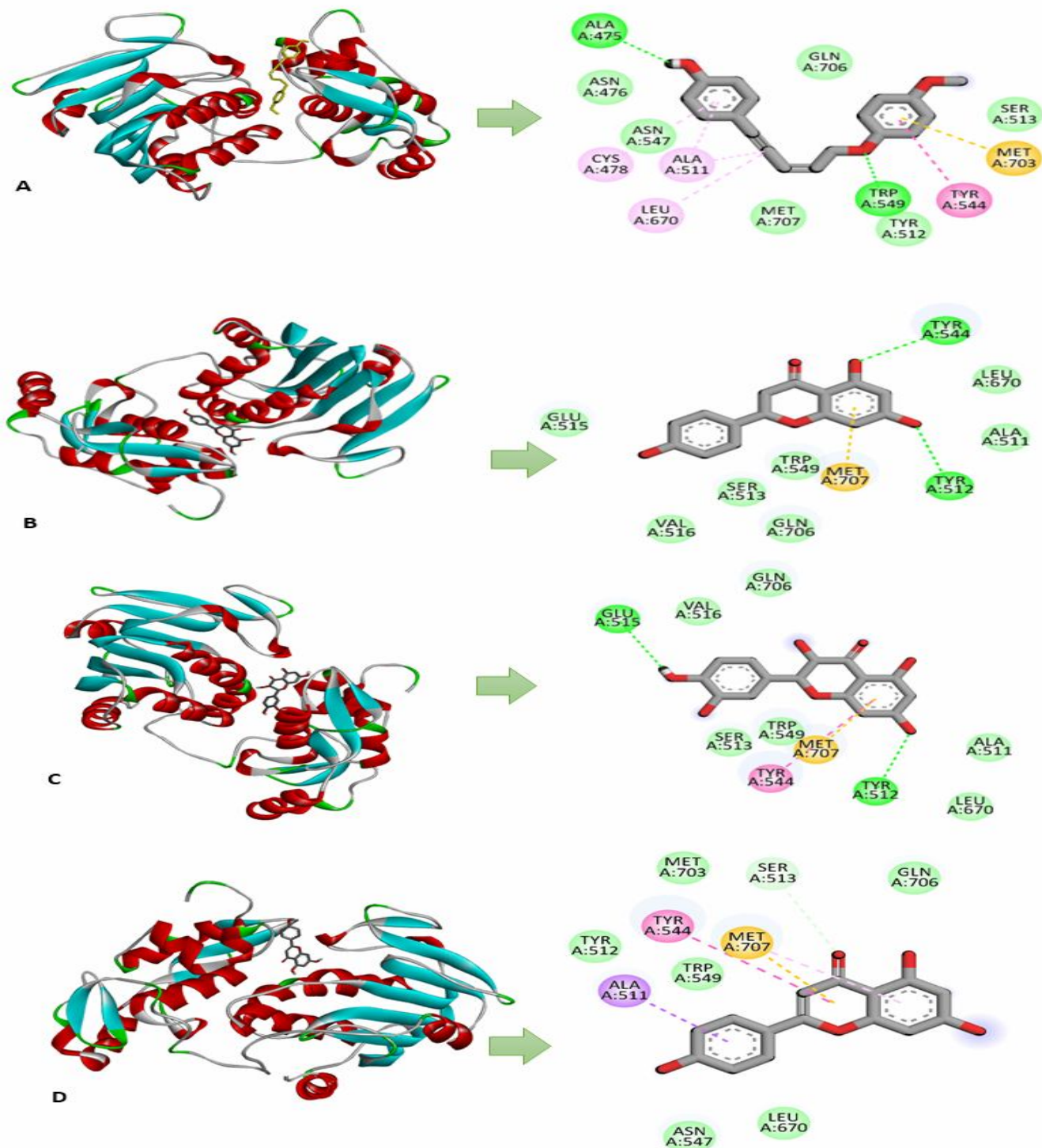
Table 2 : Type of bond interactions, number of bond and amino acid residue between best docked phytochemical with nsP2pro

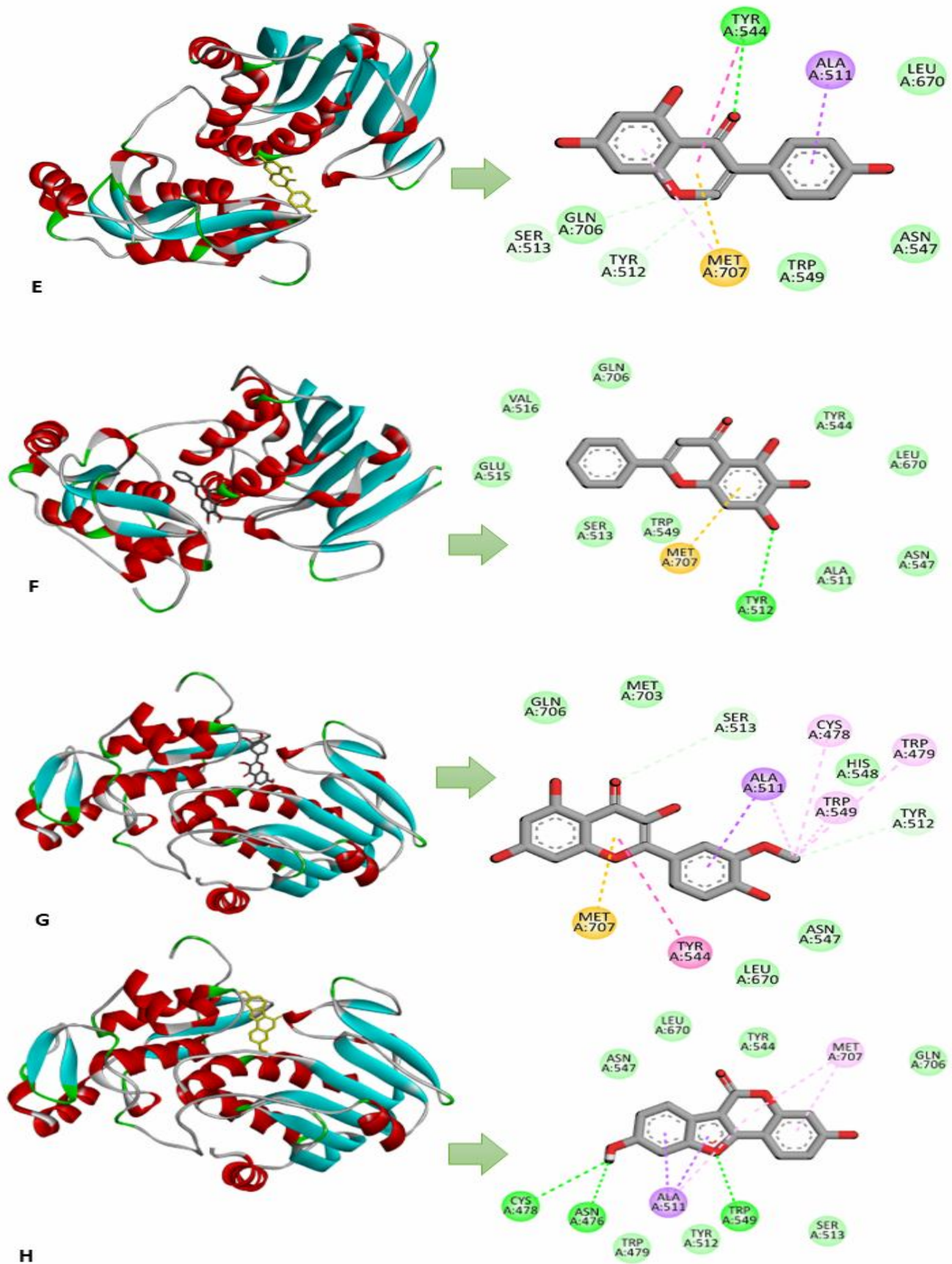
S. No.	Compound name	Pharmacological activity	Type of bond interaction	Number of bonds	Bond formed in between amino acids & ligands	References
1	Taxifolin	Antioxidant	Hydrogen Bond	2	Tyr512, Glu515	Xie <i>et al.</i> , 2017
		Anti-inflammatory	Pi-Sulfur	1	Met 707	Cai <i>et al.</i> , 2018
		Anti-Alzheimer	Pi-Pi	1	Tyr544	Saito <i>et al.</i> , 2017
2	Asparenyol	Inhibit activity Cyclooxygenase-2	Hydrogen Bond	2	Trp549, Ala475	Jang <i>et al.</i> , 2004
			Pi-Sulfur	1	Met 707	
			Pi-Pi	1	Tyr544	
			Pi-Alkyl	2	Cys478, Ala511	
			Alkyl interaction	1	Leu670	
3	Naringenin	Antiaging	Hydrogen Bond	2	Tyr544, Tyr512	Da pozzo <i>et al.</i> , 2017
		Breast cancer	Pi-Sulfur	1	Met 707	Chandrika <i>et al.</i> , 2016
4	Apigenin	Anti-cancer	Carbon-Hydrogen bond	1	Ser513	Yan <i>et al.</i> , 2017
		Antioxidant	Pi-sigma	1	Ala511	Ali <i>et al.</i> , 2014
		Antibacterial	Pi-Sulfur	1	Met 707	Teotia <i>et al.</i> , 2024
		Antifungal	Pi-Pi	1	Tyr544	Chauhan <i>et al.</i> , 2017
5	Isorhamnetin	Antiglycation activity	Carbon-Hydrogen bond	2	Ser513, Tyr512	Sindhuja <i>et al.</i> , 2023
		Anti-pulmonary fibrosis	Pi-Sigma	1	Ala511	Zhang <i>et al.</i> , 2019
		Anti-osteoporotic effect	Pi-Sulfur	1	Met 707	Chao <i>et al.</i> , 2016
		Anti-hypoxia effect	Pi-Pi	1	Tyr544	Jiang <i>et al.</i> , 2015
		Antiviral activity	Pi-Alkyl	3	Cys478, Trp479, Trp549	Dayem <i>et al.</i> , 2015
6	Genistein	Anti-Alzheimer	Hydrogen Bond	1	Tyr544	Bagheri <i>et al.</i> , 2011
		Anti-cancer	Carbon-Hydrogen bond	2	Ser513, Tyr512	Banerjee <i>et al.</i> , 2008
		Antioxidant	Pi-sigma	1	Ala511	Wei <i>et al.</i> , 1995
		Antipromotional	Pi-Sulfur	1	Met 707	Wei <i>et al.</i> , 1995
		Reduce cardiovascular risk	Pi-Pi	1	Tyr544	Atteritano <i>et al.</i> , 2007
7	Baicalein	Anti-inflammatory	Hydrogen Bond	1	Tyr512	Dinda <i>et al.</i> , 2017
		Antiviral activity	Pi-Sulfur	1	Met 707	Song <i>et al.</i> , 2021
8	Daidzein	Anticancer	Hydrogen Bond	2	Tyr544, Asn547	Singh-Gupta <i>et al.</i> , 2010
		Anti-fibrotic effect	Carbon-Hydrogen bond	2	Ser513, Tyr512	Soumyakrishnan <i>et al.</i> , 2014
		Osteogenic activity	Pi-sigma	1	Ala511	Strong <i>et al.</i> , 2014
		Neuroprotective effect	Pi-Sulfur	1	Met 707	Yang <i>et al.</i> , 2012
		increase skin collagen synthesis	Pi-Pi	1	Tyr544	Zhao <i>et al.</i> , 2015
		Effective in anxiety	Pi-Alkyl	1	Met 707	Zeng <i>et al.</i> , 2010
9	Coumestrol	Antioxidant activity	Hydrogen Bond	3	Trp549, Cys478, Asn476	Durmaz <i>et al.</i> , 2022
		Anticancer activity	Pi-sigma	1	Ala511	Lim <i>et al.</i> , 2016
		Antiobesity effects	Pi-Alkyl	1	Met 707	Kim <i>et al.</i> , 2020

Molecular docking Visualizations

To visualize 2D and 3D interactions between ligands and their target proteins using Discovery Studio software, a detailed and systematic approach is employed. Initially, the protein and ligand structures undergo energy minimization to achieve the most stable conformations. Discovery Studio facilitates the visualization of various interactions, including conventional hydrogen bonds, van der Waals

interactions, carbon-hydrogen bonds, pi-alkyl, pi-sulfur, pi-sigma, pi-anion, and alkyl interactions (Fig 2.). In 2D visualization, interaction diagrams succinctly illustrate these interactions, highlighting key residues and bonds for easy interpretation. The 3D visualization offers a comprehensive spatial perspective that allow workers to examine the ligand's fit within the protein's binding pocket and assess the overall molecular conformation.





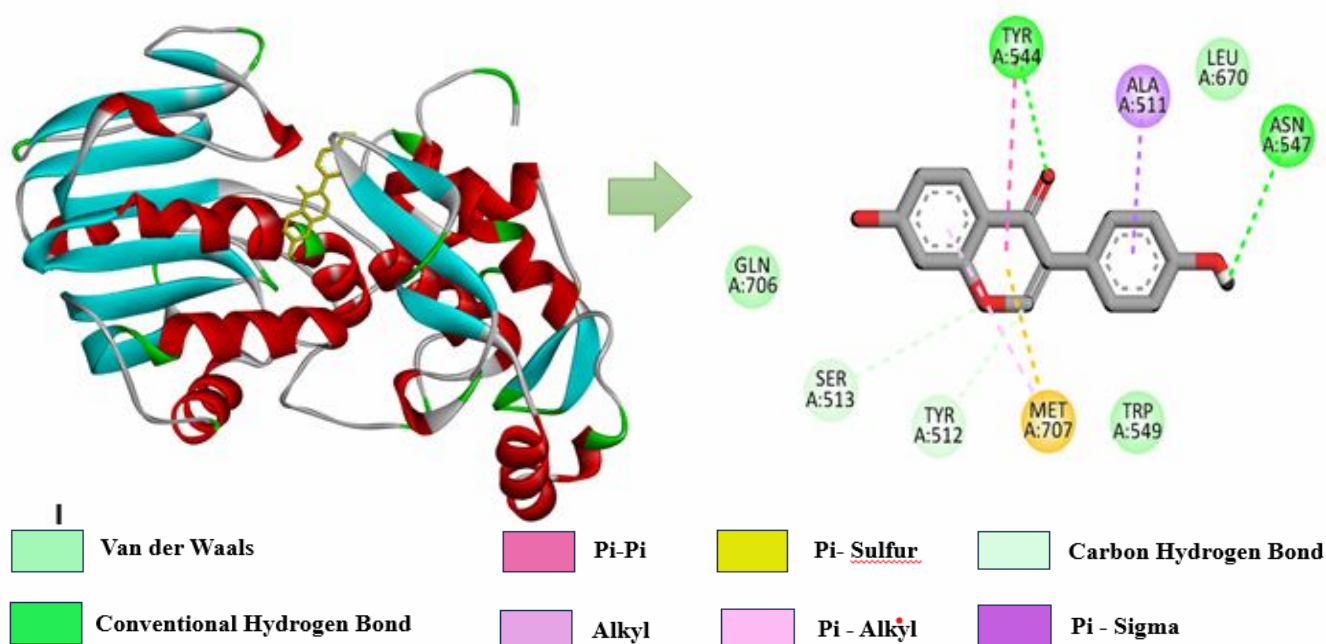


Fig. 2 : Visualization of 2D & 3D ligand-protein complexes A. asparenol, B. naringenin C. taxifolin D. apigenin E. genistein F. baicalein G. isorhamnetin H. coumestrol I. daidzein. These shows binding energy higher than -6 kcal/mol.

Molecular dynamics simulations

Additionally, MD simulations of certain phytomolecules were carried out. Proteins can experience a wide variety of conformational changes as a result of ligand interaction. Therefore, we have calculated several metrics such as Root-mean-square deviation (RMSD), Root-mean-square fluctuation (RMSF), and Radius of gyration (Rg) for free and all protein-ligand complexes in order to analyse the ligand-induced structural changes in protein and stability of protein-ligand complexes (Table 3).

Root mean square deviation

The protein RMSD computation using MD simulation help in the quantification of the potential degree of conformational changes. The RMS deviation of the C α atoms from its starting structures was calculated to elucidate the stability of complexes. The RMSD of nsP2pro C α atoms from the beginning structure fluctuates between 0.1–0.23 nm and it became stable from 10-30ns hitting the maximum at 0.59 nm in 80 ns. Fluctuations seen between 40-85 ns in RMSD plot indicate that nsP2pro showed stable conformation in the complex state. However, the mean RMSD of nsP2pro-coumestrol complex exhibited an average RMSD of 0.2 to 0.58 nm. Since the RMSD for system was less than 0.35 nm, at 90ns onwards, so it can be concluded that nsP2pro is stable in ligand-bound states. Consequently, it can be said that the enzyme's initial conformation has slightly changed

significantly throughout the simulation period and become stable below 0.35 (Fig. 3.a).

Root mean square fluctuation

The flexibility and dynamics of the system are measured by RMSF. The majority of the enzyme's residues have RMSF fluctuations that range in intensity from 0.1 to 0.5 nm. The fluctuation shows that the amino acid residues' positions are unaffected by binding of coumestrol to the active site nsP2pro. Therefore, it can be concluded that the dynamics of the protein have not been affected by ligand and protein interaction (Fig. 3.b).

Radius of gyration

The compactness & stability of the protein is determined by radius of gyration (Rg). If the value of Rg is low, then conformation protein will be stable. Rg variation was seen in every scenario over the course of the simulation because ligand interaction may cause a protein to unfold. The values of complex range from ~ 2.1 to 2.3 nm for nsP2pro bound to phytomolecules were observed. This suggests that the integrity and compactness of nsP2pro are unaffected by the binding of coumestrol to nsP2pro (Fig 3.c).

Solvent accessible surface area

The stability of globular proteins in solution is enhanced by hydrophobic interactions between non-polar amino acids, which shield these amino acids in hydrophobic cores from the aqueous environment.

Theoretically, SASA can be used to identify changes in the solvent accessibility of proteins. It gauges the free energy of solvation of every atom in the solution, including water and the polar and non-polar amino acids in proteins. In the presence of ligand, the SASA profile of protein is 155-167 nm². This indicates that protein folding is unaffected by binding to ligand to protein (Fig 3.d).

Hydrogen bond analysis

The GROMACS H-bond module was utilized to determine the hydrogen bond that was established between the bioactive metabolites and nsP2pro. Maximum hydrogen bond formation occurred between 1 to 3 in number and rarely 1-4 in number when the hydrogen bonds were disseminated in tandem with the 100 ns simulation (Fig 3.e).

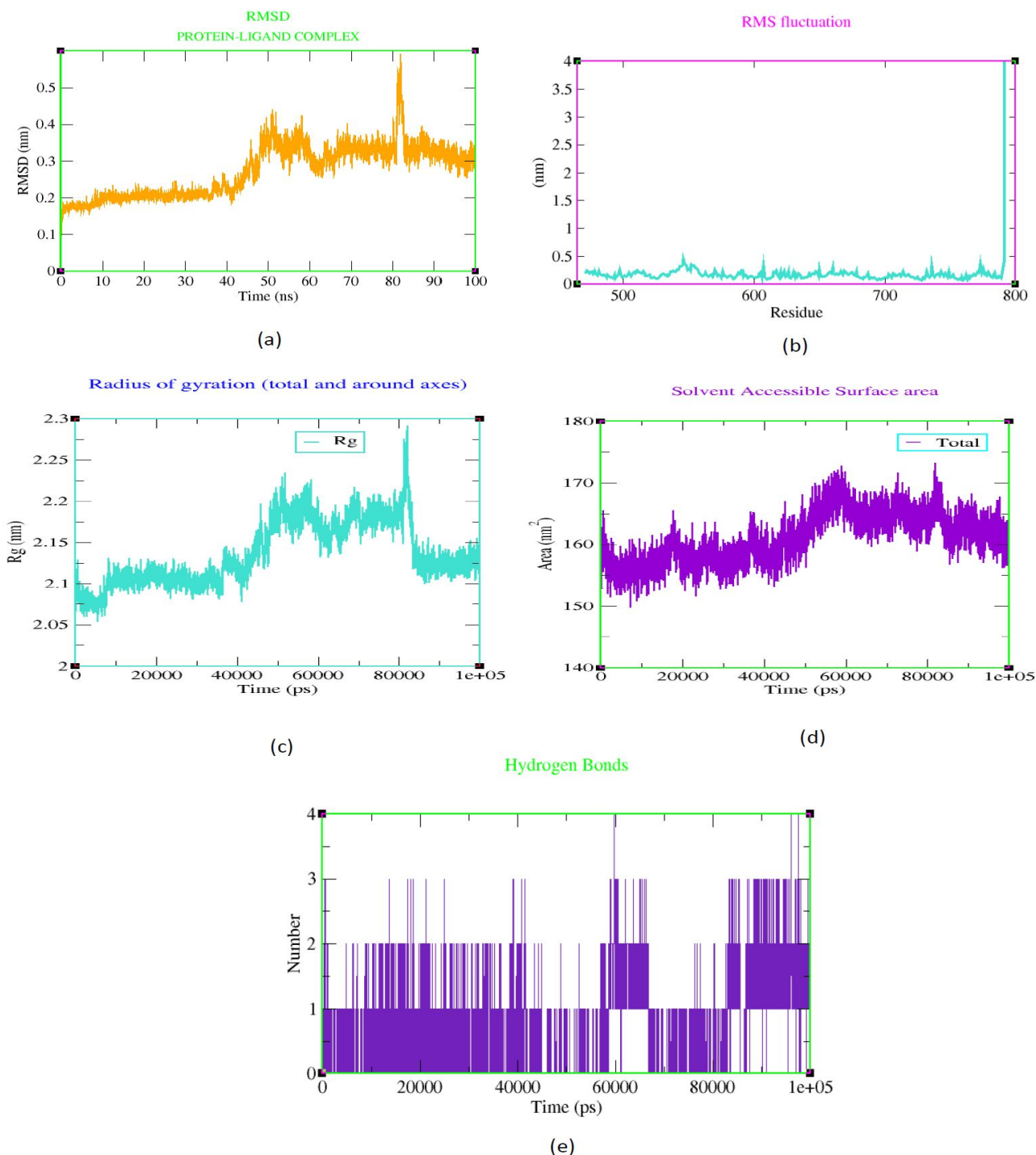


Fig. 3 : Plot of MD simulation between coumestrol-nsP2pro (a) RMSD (b) RMSF (c) Radius of gyration (d) SASA (e) H-bond.

Table 3 : Average values of different parameters using for MD simulation studies

Molecular Dynamic Parameters	Range
Complex RMSD (Root mean square deviation)	0.3 ± 0.2
Radius of gyration	2.15 ± 0.11
SASA (Solvent accessible surface area)	160 ± 10
RMSF(Root mean square fluctuation)	0.3 ± 0.2
No of hydrogen-bond	3-4

Binding free energy calculation

MMPBSA analysis that represents the ligands' binding potential was used to compute the binding free energy (ΔG_{bind}). The MMPBSA results indicate that coumestrol molecule forms a stable complex by binding to the nsP2pro active site which is represented by the least binding free energy hence maximum affinity with nsP2pro. Lower binding free energy is largely caused by the difference in ΔG_{bind} , which is primarily caused by the ΔE_{vdw} (energy of van der Waals interactions) interaction component and ΔG_{solv} free energy components. The binding free energy of enzyme-ligand complex was influenced by a number of energy components, including electrostatic energy (EEL), polar solvation energy (ΔG_{psolv}), nonpolar solvation energy (ΔG_{npolv}), and van der Waals energy (ΔE_{vdw}). The ligands' MMPBSA results were provided (table 4).

Table 4 : MMPBSA energy of protein ligand-complex (kJ/mol)

S. No.	Different Energies	Coumestrol
1	$\Delta E_{\text{VDWAALS}}$	-29.69 ± 0.44
2	ΔE_{EL}	1.90 ± 2.63
3	ΔE_{PB}	16.53 ± 2.77
4	ΔE_{NPOLAR}	-2.92 ± 0.04
5	ΔG_{GAS}	-27.78 ± 2.60
6	ΔG_{SOLV}	13.61 ± 2.75
7	ΔT_{Total}	-14.17 ± 1.57

Results

According to drug likeliness, molecular docking, molecular dynamics simulation characteristics, and MMPBSA analyses, Coumestrol of *A. officinalis* has the potential to inhibit the activity of nsP2pro for chikungunya virus drug development. This inhibition is based on their high binding scores, stability of the selected bioactive metabolite complexes, and high binding free energy values.

Conclusion

In this study, the antiviral potential of bioactive metabolites from *A. officinalis* and *A. racemosus* against Chikungunya virus was investigated using an

In silico approach. The molecular docking analysis revealed that among the 36 metabolites screened, nine showed the highest binding affinity against nsP2 protease, with binding energies ranging from -6.3 to -6.8 kcal/mol. These compound (taxifolin, asparenol, naringenin, apigenin, and isorhamnetin, genistein, baicalein, daidzein, and coumestrol) demonstrating the strongest binding interactions with nsP2 protease. The findings suggest that Coumestrol shows highest binding energy (-6.8 kcal/mol) that interact with critical residues of the nsP2 protease, such as Trp549, Cys478, Asn476, Ala511, Met 707 through various interactions including hydrogen bonds, Pi-sigma, and Pi-Alkyl respectively. However, coumestrol has not yet been reported as an antiviral compound. Molecular dynamics (MD) simulations and MMPBSA (Molecular Mechanics Poisson-Boltzmann Surface Area) free energy calculations further validated the stability and binding efficiency of Coumestrol and nsP2pro protein complex. In our finding, Coumestrol of *A. officinalis* has emerged as the most promising novel compound due to its high binding score and stability, indicating its potential to inhibit the activity of nsP2 protease effectively for chikungunya virus drug development. This study states the potential of *Asparagus officinalis* root-derived phytochemicals as antiviral agents against Chikungunya virus, providing us the way for further experimental validation and potential therapeutic development. Given the lack of effective treatments or vaccines for Chikungunya, these findings hold significant promise for developing novel antiviral therapies.

Acknowledgement

Authors extend heartfelt gratitude to head department of Botany Chaudhary Charan Singh University, Meerut for providing facility & UGC-CSIR for providing financial assistance.

Data availability: All supplementary files are available with first author (Aman Agrawal).

References

- Agrawal, S., Prakash, R., Dixit, A. and Srivastava, A. (2018). Chemical Analysis and their Therapeutic activity of Ethanolic extract of *Asparagus racemosus* (Shatawari) Root by GC-MS analysis. *J. Ultra Chem.*, **14**(6), 163.
- Ali, F., Naz, F., Jyoti, S. and Siddique, Y.H. (2014). Protective effect of apigenin against N-nitrosodiethylamine (NDEA)-induced hepatotoxicity in albino rats. *Mutat. Res./Genet. Toxicol. Environ. Mutagen.*, **767**: 13-20.
- Atteritano, M., Marini, H., Minutoli, L., Polito, F., Bitto, A., Altavilla, D. and Squadrito, F., (2007). Effects of the phytoestrogen genistein on some predictors of cardiovascular risk in osteopenic, postmenopausal women: a two-year randomized, double-blind, placebo-

- controlled study. *J. Clin. Endocrinol. Metab.*, **92**(8), 3068-3075.
- Bagheri, M., Joghataei, M.T., Mohseni, S. and Roghani, M. (2011). Genistein ameliorates learning and memory deficits in amyloid β (1–40) rat model of Alzheimer's disease. *Neurobiol. Learn. Mem.*, **95**(3), 270-276.
- Bajpai, V., Singh, P., Chandra, P. and Kumar, B. (2022). *Asparagus Sp.: Phytochemicals and Marketed Herbal Formulations*. In: *Medicinal Plants*, Apple Academic Press, pp. 299-318.
- Banerjee, S., Li, Y., Wang, Z. and Sarkar, F.H. (2008). Multi-targeted therapy of cancer by genistein. *Cancer Lett.*, **269**(2), 226-242.
- Berendsen, H.J., Postma, J.V., Van Gunsteren, W.F., DiNola, A.R.H.J. and Haak, J.R. (1984). Molecular dynamics with coupling to an external bath. *J. Chem. Phys.*, **81**(8), 3684-3690.
- Bongirwar, A. A. and Tirgar, P. (2023). Anticancer activity of nanosuspension of ethanolic extracts of leaves of *Asparagus racemosus*. *Int. J. Med. Toxicol. Legal Med.*, **26**(1&2), 38.
- Bopana, N. and Saxena, S. (2007). *Asparagus racemosus*: Ethnopharmacological evaluation and conservation needs. *J. Ethnopharmacol.*, **110**(1), 1-15.
- Cai, C., Liu, C., Zhao, L., Liu, H., Li, W., Guan, H. and Xiao, J. (2018). Effects of Taxifolin on Osteoclastogenesis in vitro and in vivo. *Front. Pharmacol.*, **9**, 1286.
- Cecilia, D. (2014). Current status of dengue and chikungunya in India. *WHO South-East Asia J. Public Health*, **3**(1), 22-27.
- Chandrika, B. B., Steephan, M., Kumar, T. S., Sabu, A. and Haridas, M., (2016). Hesperetin and naringenin sensitize HER2 positive cancer cells to death by serving as HER2 tyrosine kinase inhibitors. *Life Sci.*, **160**: 47-56.
- Chao, G., Liao, S. and Zhou, J. (2016). Anti-osteoporotic effect and mechanism of isorhamnetin against ovariectomy-induced osteoporosis in rats. *Chin. Hosp. J. Pharm.*, **36**: 1456-1460.
- Chauhan, D., Husain, N. and Trak, T.H. (2017). Ethnomedicinal and pharmacognostical studies of some traditionally important medicinal plants from three districts of Chhattisgarh, India. *Indian J. Sci. Res.*, **15**(1), 69-76.
- Da Pozzo, E., Costa, B., Cavallini, C., Testai, L., Martelli, A., Calderone, V. and Martini, C. (2017). The citrus flavanone Naringenin protects myocardial cells against age - associated damage. *Oxid. Med. Cell. Longev.*, **2017**(1), 9536148.
- Dayem, A.A., Choi, H.Y., Kim, Y.B. and Cho, S.G. (2015). Antiviral effect of methylated flavonol isorhamnetin against influenza. *PLoS One*, **10**(3), e0121610.
- Design, L. (2014). Pharmacophore and ligand-based design with Biovia Discovery Studio®. *BIOVIA*, California.
- Dhanusha, G., Sujith, S., Nisha, A.R., Aathira, K.K. and Haima, J.S. (2021). Cytotoxic and antiproliferative potential of methanolic extracts of *Asparagus racemosus* in MDAMB231 cells. *Pharma Innov. J.*, **10**(2), 355-358.
- Dinda, B., Dinda, S., DasSharma, S., Banik, R., Chakraborty, A. and Dinda, M. (2017). Therapeutic potentials of baicalin and its aglycone, baicalein against inflammatory disorders. *Eur. J. Med. Chem.*, **131**, 68-80.
- Durmaz, L., Erturk, A., Akyüz, M., Polat Kose, L., Uc, E. M., Bingol, Z. and Gulcin, İ. (2022). Screening of carbonic anhydrase, acetylcholinesterase, butyrylcholinesterase, and α -glycosidase enzyme inhibition effects and antioxidant activity of coumestrol. *Molecules*, **27**(10), 3091.
- Fros, J.J., Liu, W.J., Prow, N.A. et al. (2010). Chikungunya virus nonstructural protein 2 inhibits type I/II interferon-stimulated JAK-STAT signaling. *J. Virol.*, **84**, 10877-10887.
- Farnsworth, N.R., Akerele, O., Bingel, A.S., Soejarto, D.D. and Guo, Z. (1985). Medicinal plants in therapy. *Bull. World Health Organ.*, **63**(6), 965.
- Guex, N. and Peitsch, M.C. (1997). Swiss-Model and the Swiss - Pdb Viewer: an environment for comparative protein modeling. *Electrophoresis*, **18**(15), 2714-2723.
- Hamdi, A., Jaramillo-Carmona, S., Rodríguez-Arcos, R., Jiménez-Araujo, A., Lachaal, M., Karray-Bourouai, N. and Guillén-Bejarano, R. (2021). Phytochemical characterization and bioactivity of *Asparagus racemosus*: A focus on antioxidant, cytotoxic, lipase inhibitory and antimicrobial activities. *Molecules*, **26**(11), 3328.
- Hartung, A.C., Nair, M.G. and Putnam, A.R. (1990). Isolation and characterization of phytotoxic compounds from *Asparagus officinalis* roots. *J. Chem. Ecol.*, **16**: 1707-1718.
- Hasan, N., Ahmad, N., Zohrameena, S., Khalid, M. and Akhtar, J. (2016). *Asparagus racemosus*: for medicinal uses & pharmacological actions. *Int. J. Adv. Res.*, **4**(3), 259-267.
- Hess, B., Bekker, H., Berendsen, H.J. and Fraaije, J.G., (1997). LINCOS: a linear constraint solver for molecular simulations. *J. Comput. Chem.*, **18**(12), 1463-1472.
- RCSB PDB, (Accessed on December 20, 2022). Available at: <http://www.rcsb.org/pdb/home/home.do>
- Ito, T., Sato, A., Ono, T., Goto, K., Maeda, T., Takanari, J. et al. (2013). Isolation, structural elucidation, and biological evaluation of a 5-hydroxymethyl-2-furfural derivative, asfural, from enzyme-treated asparagus extract. *J. Agric. Food Chem.*, **61**(38), 9155-9159.
- Jang, D.S., Cuendet, M., Fong, H.H., Pezzuto, J.M. and Kinghorn, A.D., (2004). Constituents of *Asparagus officinalis* evaluated for inhibitory activity against cyclooxygenase-2. *J. Agric. Food Chem.*, **52**(8), 2218-2222.
- Jain, P., Kumar, V., Teotia, D., Goyal, H., Agrawal, A. and Malik, V., (n.d.). Phytochemical Composition of *Sida rhombifolia* Ssp. *retusa* (L.) Bross.: A Comprehensive GC/MS Analysis. DOI: 10.5281/zenodo.10578898
- Ji, K., Kim, Y.E. and Kim, Y.T. (2016). Anti-oxidative Effects of *Asparagus officinalis* Extracts. *Korean Soc. Food Nutr. Conf. Proc.*: 432-432.
- Jiang, L., Mo, H. and Zhang, Z., (2015). Experimental study on the anti-hypoxia effect of isorhamnetin under different hypoxia conditions. *J. Northwest Univ. Natl. (Nat. Sci. Ed.)*, **36**(03), 38-41.
- Kadhim, E.J. and Salah, Z. (2014). Phytochemical investigation & antibacterial activity of the essential oils from two species of *Asparagus* cultivated in Iraq. *Pharmacie Globale*, **5**(3), 1-4.
- Karthikeyan, M., Karthikeyan, B.S., Vivek-Ananth, R.P., Chand, R.B., Aparna, S.R., Pattulingam, M. and Areejit, S. (2018). IMPPAT: a curated database of Indian Medicinal Plants, phytochemistry and therapeutics. *Sci. Rep.*, **8**(1).

- Kim, S.N., Ahn, S.Y., Song, H.D., Kwon, H.J., Saha, A., Son, Y. and Lee, Y.H. (2020). Antiobesity effects of coumestrol through expansion and activation of brown adipose tissue metabolism. *J. Nutr. Biochem.*, **76**: 108300.
- Kim, S., Chen, J., Cheng, T., Gindulyte, A., He, J., He, S. and Bolton, E.E. (2019). PubChem 2019 update: improved access to chemical data. *Nucleic Acids Res.*, **47**(D1), D1102-D1109.
- Kumar, S., Choudhir, G., Sharma, S., Vimala, Y., Joshi, N., Tiwari, A. et al. (2023). Computational probing of *Nigella sativa* bioactive metabolites against *Chikungunya* nsP2 cysteine protease. *J. King Saud Univ. Sci.*, **35**(4), 102651.
- Kumar, S., Srivastava, P., Gupta, S., Dhanawat, M., Rani, S., Ajiboye, B. O. and Gautam, R. K., (2023). Pharmacological evaluation of different extracts of *Asparagus officinalis* as an analgesic, anti-inflammatory and anti-arthritic agent in rats. *Pharmacogn. Res.*, **15**(1), 184-205.
- Kumari, R., Kumar, R., Consortium, O. and Lynn, A. (2014). g_mmpbsa – A GROMACS tool for high-throughput MM-PBSA calculations. *J. Chem. Inf. Model.*, **54**(7), 1951–1962.
- Lim, W., Jeong, W. and Song, G. (2016). Coumestrol suppresses proliferation of ES2 human epithelial ovarian cancer cells. *J. Endocrinol.*, **228**(3), 149-160.
- Lipinski, C.A., Lombardo, F., Dominy, B.W. et al. (1997). Experimental and computational approaches to estimate solubility and permeability in drug discovery and development settings. *Adv. Drug Deliv. Rev.*, **23**(1–3), 3–25.
- López, G., Ros, G., Rincón, F., Ortuno, J., Periago, M.J. and Martínez, M.C., (1996). Amino acids and in vitro protein digestibility changes in green asparagus (*Asparagus officinalis*, L.) during growth and processing. *Food Res. Int.*, **29**(7), 617-625.
- Morris, G.M., Huey, R., Lindstrom, W., Sanner, M.F., Belew, R.K., Goodsell, D.S. and Olson, A.J., (2009). AutoDock4 and AutoDockTools4: Automated docking with selective receptor flexibility. *J. Comput. Chem.*, **30**(16), 2785-2791.
- Narwal, M., Singh, H., Pratap, S. et al. (2018). Crystal structure of chikungunya virus nsP2 cysteine protease reveals a putative flexible loop blocking its active site. *Int. J. Biol. Macromol.*, **116**: 451–462.
- O'Boyle, N.M., Banck, M., James, C.A., Morley, C., Vermeersch, T. and Hutchison, G.R., (2011). Open Babel: An open chemical toolbox. *J. Cheminform.*, **3**(1), 33.
- Rauf, M., Manzoor, S., Mehmood, A. and Bhatti, S., (2017). Outbreak of chikungunya in Pakistan. *Lancet Infect. Dis.*, **17**(3), 258.
- Rikonen, M., (1996). Functional significance of the nuclear-targeting and NTP-binding motifs of Semliki Forest virus nonstructural protein nsP2. *Virology*, **218**(2), 352-361.
- Robinson, M.C. (1955). An epidemic of virus disease in Southern Province, Tanganyika territory, in 1952–1953. *Trans. R. Soc. Trop. Med. Hyg.*, **49**(1), 28-32.
- Ross, R.W. (1956). The Newala epidemic: III. The virus: isolation, pathogenic properties and relationship to the epidemic. *Epidemiol. Infect.*, **54**(2), 177-191.
- Saito, S., Yamamoto, Y., Maki, T., Hattori, Y., Ito, H., Mizuno, K. et al. (2017). Taxifolin inhibits amyloid- β oligomer formation and fully restores vascular integrity and memory in cerebral amyloid angiopathy. *Acta Neuropathol. Commun.*, **5**: 1-16.
- Sharma, S.C., Sharma, R. and Kumar, R. (1983). Spirostanosides of *Asparagus sprengeri*. *Phytochemistry*, **22**(10), 2259-2262.
- Sindhuja, A., Vimalavathini, R., Velu, K.V. and Vickneshwaran, V. (2023). In vitro antiglycation activity of isorhamnetin on bovine serum albumin with different sugars using sodium dodecyl sulphate polyacrylamide gel electrophoresis. *Res. J. Pharm. Technol.*, **16**(8), 3525-3529.
- Singh, A., Kumar, A., Uversky, V.N. and Giri, R. (2018). Understanding the interactability of chikungunya virus proteins via molecular recognition feature analysis. *RSC Adv.*, **8**(48), 27293-27303.
- Singh-Gupta, V., Zhang, H., Yunker, C.K., Ahmad, Z., Zwier, D., Sarkar, F.H. and Hillman, G.G. (2010). Daidzein effect on hormone refractory prostate cancer in vitro and in vivo compared to genistein and soy extract: potentiation of radiotherapy. *Pharm. Res.*, **27**: 1115-1127.
- Sivakumar, T. and Gajalakshmi, D. (2014). Phytochemical screening and GC-MS analysis of root extract from *Asparagus racemosus* L. *Int. J. Pharm. Sci. Res.*, **5**(12), 5245.
- Song, J., Zhang, L., Xu, Y., Yang, D., Yang, S., Zhang, W. and Du, G. (2021). The comprehensive study on the therapeutic effects of baicalein for the treatment of COVID-19 in vivo and in vitro. *Biochem. Pharmacol.*, **183**: 114302.
- Soumyakrishnan, S., Divya, T., Kalayarasan, S., Sriram, N. and Sudhandiran, G. (2014). Daidzein exhibits anti-fibrotic effect by reducing the expressions of Proteinase activated receptor 2 and TGF β 1/smad mediated inflammation and apoptosis in Bleomycin-induced experimental pulmonary fibrosis. *Biochimie*, **103**: 23-36.
- Janani, S.R. and Singaravadiel, K. (2014). Screening of phytochemical and GC-MS analysis of some bioactive constituents of *Asparagus racemosus*. *Screening*, **6**(2), 428-432.
- Strong, A.L., Ohlstein, J.F., Jiang, Q., Zhang, Q., Zheng, S., Boue, S.M. and Bunnell, B.A. (2014). Novel daidzein analogs enhance osteogenic activity of bone marrow-derived mesenchymal stem cells and adipose-derived stromal/stem cells through estrogen receptor dependent and independent mechanisms. *Stem Cell Res. Ther.*, **5**: 1-17.
- Sun, T., Powers, J.R. and Tang, J. (2007). Evaluation of the antioxidant activity of *Asparagus*, broccoli and their juices. *Food Chem.*, **105**(1), 101-106.
- SwissADME: a free web tool to evaluate pharmacokinetics, drug-likeness and medicinal chemistry friendliness of small molecule, (2017). *Sci. Rep.*, **7**: 42717.
- Teotia, D., Agrawal, A., Goyal, H., Jain, P., Singh, V., Verma, Y. et al. (2024). Pharmacophylogeny of genus *Allium* L. *J. King Saud Univ. Sci.*, **36**(8), 103330.
- Terada, K. and Kamisako, W., (1999). 1H-NMR and Mass Spectral Study of a D-Enriched Acetylenic Norlignan, Asparenol, from Cultured Cells of *Asparagus officinalis*. *Biol. Pharm. Bull.*, **22**(6), 561-566.
- Thakur, A.V., Ambwani, T.K., Ahmad, A.H., Rawat, D.S. and Ambwani, S., (2018). Determination of the phytochemical ingredients and antioxidative potential of hydromethanolic

- extract of *Asparagus racemosus* Willd. *Int. J. Herb. Med.*, **6**(1), 39-43.
- Tomasello, D. and Schlagenhauf, P. (2013). Chikungunya and dengue autochthonous cases in Europe, 2007–2012. *Travel Med. Infect. Dis.*, **11**(5), 274-284.
- Trott, O. and Olson, A.J., (2010). AutoDock Vina: improving the speed and accuracy of docking with a new scoring function, efficient optimization, and multithreading. *J. Comput. Chem.*, **31**(2), 455–461.
- Van Bortel, W., Dorleans, F., Rosine, J., Blateau, A., Rousset, D., Matheus, S. *et al.* (2014). Chikungunya outbreak in the Caribbean region, December 2013 to March 2014, and the significance for Europe. *Euro Surveill.*, **19**(13), 20759.
- Van Der Spoel, D., Lindahl, E., Hess, B., Groenhof, G., Mark, A.E. and Berendsen, H.J., (2005). GROMACS: fast, flexible and free. *J. Comput. Chem.*, **26**(16), 1701–1718.
- Vanommeslaeghe, K., Hatcher, E., Acharya, C., Kundu, S., Zhong, S., Shim, J. *et al.* (2010). CHARMM general force field: A force field for drug - like molecules compatible with the CHARMM all - atom additive biological force fields. *J. Comput. Chem.*, **31**(4), 671-690.
- Wei, H., Bowen, R., Cai, Q., Barnes, S. and Wang, Y., (1995). Antioxidant and antipromotional effects of the soybean isoflavone genistein. *Proc. Soc. Exp. Biol. Med.*, **208**(1), 124-130.
- Xie, X., Feng, J., Kang, Z., Zhang, S., Zhang, L., Zhang, Y. and Tang, Y., (2017). Taxifolin protects RPE cells against oxidative stress-induced apoptosis. *Mol. Vis.*, **23**: 520-528.
- Yan, X., Qi, M., Li, P., Zhan, Y. and Shao, H., (2017). Apigenin in cancer therapy: Anti-cancer effects and mechanisms of action. *Cell Biosci.*, **7**: 1-16.
- Yang, C., Ye, Z., Mao, L., Zhang, L., Zhang, J., Ding, W. *et al.* (2022). Analysis of volatile organic compounds and metabolites of three cultivars of *Asparagus officinalis* L. using E-nose, GC-IMS, and LC-MS/MS. *Bioengineered*, **13**(4), 8866-8880.
- Yang, S.H., Liao, C.C., Chen, Y., Syu, J.P., Jeng, C.J. and Wang, S.M., (2012). Daidzein induces neuritogenesis in DRG neuronal cultures. *J. Biomed. Sci.*, **19**: 1-13.
- Zeng, S., Tai, F., Zhai, P., Yuan, A., Jia, R. and Zhang, X., (2010). Effect of daidzein on anxiety, social behavior and spatial learning in male Balb/cJ mice. *Pharmacol. Biochem. Behav.*, **96**(1), 16-23.
- Zhang, H., Birch, J., Pei, J., Mohamed Ahmed, I.A., Yang, H., Dias, G. *et al.* (2019). Identification of six phytochemical compounds from *Asparagus officinalis* L. root cultivars from New Zealand and China using UAE-SPE-UPLC-MS/MS: effects of extracts on H₂O₂-induced oxidative stress. *Nutrients*, **11**(1), 107.
- Zhang, M., Zhao, G., Zhang, G., Wei, X., Shen, M., Liu, L., Ding, X. and Liu, Y. (2020). A targeted analysis of flavonoids in asparagus using the UPLC-MS technique. *Czech J. Food Sci.*, **38**: 77–83.
- Zhao, D., Shi, Y., Dang, Y., Zhai, Y. and Ye, X. (2015). Daidzein stimulates collagen synthesis by activating the TGF - β /smad signal pathway. *Australas. J. Dermatol.*, **56**(1), e7-e14.